Inner filter effect: Phase relationships between oscillatory fluorescence and oscillatory Ru(II) concentration in the Belousov–Zhabotinsky reaction

Gunn Marit Solli[a] and Peter Ruoff[b]
Department of Physical Chemistry, Norwegian Institute of Technology, 7034 Trondheim, Norway, and School of Technology and Science, Stavanger College, 4004 Stavanger, Norway

(Received 9 February 1995; accepted 20 April 1995)

The oscillatory fluorescence of the Ru-ion-catalyzed Belousov–Zhabotinsky reaction has been studied and analyzed in relation to the fluorimetric behavior of the isolated $Ru(bpy)_3^{2+}$ ion. Here we show how different forms of fluorescence oscillations, observed at various excitation wavelengths and $Ru(bpy)_3^{2+}$ concentrations are due to an inner filter effect of the isolated $Ru(bpy)_3^{2+}$ ion. Three types of phase relationships, i.e., in-phase, opposite-phase, and complex phase relationships, between oscillatory fluorescence and the oscillatory $Ru(bpy)_3^{2+}$ concentration can be predicted and have experimentally been observed. © *1995 American Institute of Physics.*

I. INTRODUCTION

The Belousov[1]–Zhabotinsky[2] (BZ) reaction[3] is the metal-ion catalyzed oxidation and bromination of an organic substrate (mostly used is malonic acid) by bromate in a sulfuric acid solution. Even in batch, the BZ medium can exhibit a variety of phenomena often observed in biological systems, including excitability,[4] pulse propagation,[5] bistability,[6] and a variety of complex oscillatory behavior[7] and also chaos/irregular behavior.[8]

The chemical mechanism of the BZ reaction is quite well understood, notably due to the cornerstone work by Field, Körös, and Noyes (FKN).[9] A mathematical skeleton of the FKN (Ref. 9) mechanism, the so-called Oregonator,[10] much refined during the last years,[11] is able to simulate most of the dynamic behaviors that have been observed experimentally.

Oscillations are often recorded electrochemically, either by monitoring the bromide ion concentration with a bromide ion selective electrode or by measuring the redox potential with a platinum electrode. Spectrophotometry is also used, because the metal-ion catalysts form often colored complexes with a variety of ligands. The oscillations may become quite spectacular when $[Ru(bpy)_3]^{2+}$ is used as the catalyst and the reaction solution is illuminated with UV-light in a dark room.[12] In this case the oscillations are seen as the periodic alternations between orange fluorescence and darkness. Also pattern formations in thin unstirred layers due to the light-sensitivity of the Ru-ion have been observed and may even temporarily store graphical information.[13]

When electrochemical or spectrophotometric recorded oscillations are compared with corresponding oscillations followed by fluorimetry, the fluorimetric records can show deviations in the shape of the oscillations.[14] The reason for such deviations is not understood.

In this paper we show that various fluorescent oscillatory waveforms which deviate in form from their corresponding concentration oscillations are due to an inner filter effect that can be observed in isolated $[Ru(bpy)_3]^{2+}$ solutions. From the inner filter effect curve three types of fluorescence oscillations can be predicted[15] and which have now experimentally been observed. We denote them as in-phase, out-of-phase, and intermediate type of phase relations between oscillatory

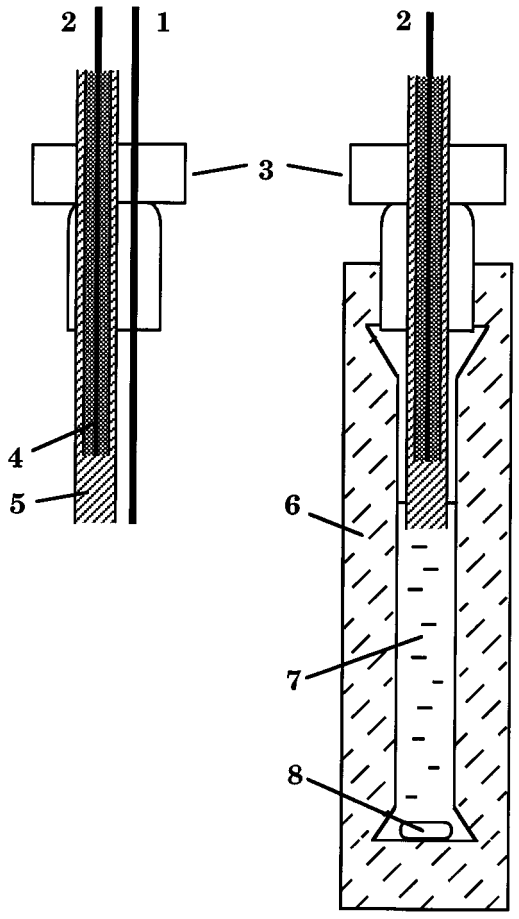

FIG. 1. Sketch of fluorimetric cell with Pt-electrode and capillary double-junction gel Ag/AgCl reference electrode. Left: side view; right: frontal view with cell. 1, Pt-wire; 2, Ag-wire of reference electrode; 3, Teflon stopper; 4, inner glass capillary (1.3 mm diam) with Ag-wire in 1% Agarose gel in half-saturated KCl; 5, outer capillary (2.4 mm diam) with 2.5% Agarose gel in half-saturated KNO_3 solution; 6, body of cell made of quartz glass (Suprasil, Heraeus Quarzglas GmbH, Germany; 7, 1.5 mℓ of reacting solution; 8, stirring bar.

[a]Norwegian Institute of Technology.
[b]To whom correspondence should be addressed at Stavanger College.

 0021-9606/95/103(4)/1440/8/$6.00

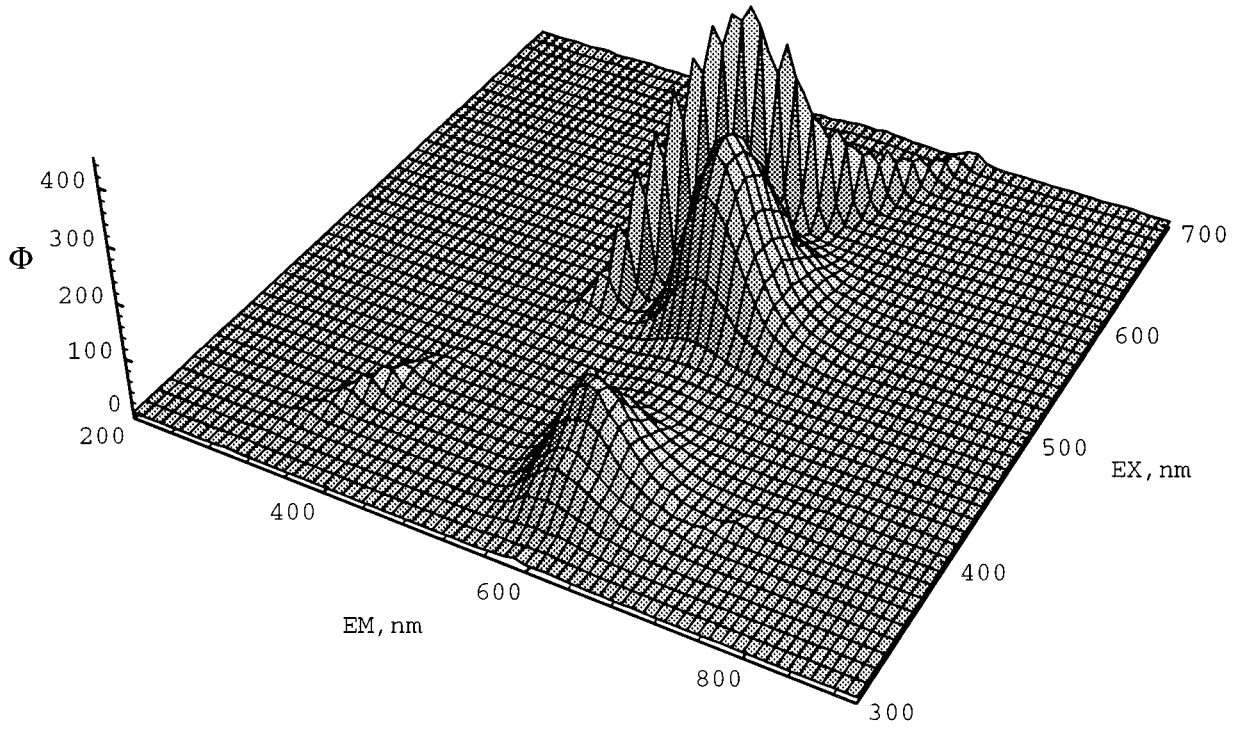

FIG. 2. Three-dimensional fluorescence spectrum of 5×10^{-4} M $Ru(bpy)_3^{2+}$ in 1 M sulfuric acid. EM and EX denote emission- and excitation wavelengths λ_{em} and λ_{ex}, respectively. The two peaks in front (at $\lambda_{em}\approx600$ nm) are the fluorescence peaks. The third peak in the back (along the line $\lambda_{em}=\lambda_{ex}$) is due to Rayleigh scattering.

fluorescence and the oscillatory $[Ru(bpy)_3]^{2+}$ concentration.

II. MATERIALS AND METHODS

A. Chemicals

All chemicals used are commercially available. With the exception of $[Ru(bpy)_3]Cl_2\cdot6H_2O$ (Aldrich, USA), all chemicals were used without further purification. Since Cl^- can inhibit[16] BZ oscillations, $[Ru(bpy)_3]Cl_2\cdot6H_2O$ was also recrystallized into the corresponding sulfate salt by adding 1 mℓ of a 5 M sulfuric acid dropwise into a saturated aqueous $[Ru(bpy)_3]Cl_2$ solution. The precipitated sulfate salt was separated by filtration and was further purified by washing with ethanol and finally with diethylether.[17] The yield of $[Ru(bpy)_3]SO_4$ formed by this procedure was about 10%. However, due to the low catalyst concentrations applied in our experiments, we did not find significant differences in shape of oscillations or in the quenching behavior (decrease of amplitude of the fluorescence oscillations) when chloride or sulfate salt was used.

All oscillators were run at 25 °C (±0.1°) in a 1 M sulfuric acid with an initial malonic acid (Koch-Light, England) concentration of 0.3 M and an initial $NaBrO_3$ (Merck, Germany) concentration of 0.1 M. The initial $[Ru(bpy)_3]^{2+}$ concentration was varied in the range 1×10^{-5} M–5×10^{-4} M.

B. Experimental techniques

Fluorescence intensities were measured in a spectrofluorimeter (Hitachi F-4500, Japan) with magnetic stirring in the cuvette. The cell and excitation/emission beam arrangement has a standard orthogonal design.[18,19] The fluorimeter was interfaced to a personal computer (PC) and spectra or time measurement data were recorded and stored on disk.

Redox potentials of the oscillatory system were recorded simultaneously with the measurement of fluorescence. For this purpose a capillary Ag/AgCl double-junction gel-electrode was made for use in the fluorimetric cell. A schematic picture of the cell (Hellma, Germany) with the capillary reference electrode is shown in Fig. 1. As a working electrode a Pt-wire was used. The redox oscillations were recorded digitally by means of a data acquisition board (Lab PC+, National Instruments, USA) and stored on a disk.

C. Computations

Double-precision computations were performed on a PC by integrating the rate equations of the Oregonator model with the FORTRAN subroutine LSODE.[20]

III. RESULTS AND DISCUSSION

A. Fluorescence behavior of the isolated $[Ru(bpy)_3]^{2+}$ ion

Figure 2 shows the fluorescence spectrum of 5×10^{-4} M $Ru(bpy)_3^{2+}$ in 1 M sulfuric acid. The same spectrum is observed in the oscillatory BZ reaction (using the same initial Ru-ion concentration) except that in the BZ reaction the heights of the fluorescence peaks oscillate (the oscillatory behavior of these peaks is described in the next section).

When studying how the fluorescence emission intensity Φ depends on the $[Ru(bpy)_3]^{2+}$ ion concentration an inner

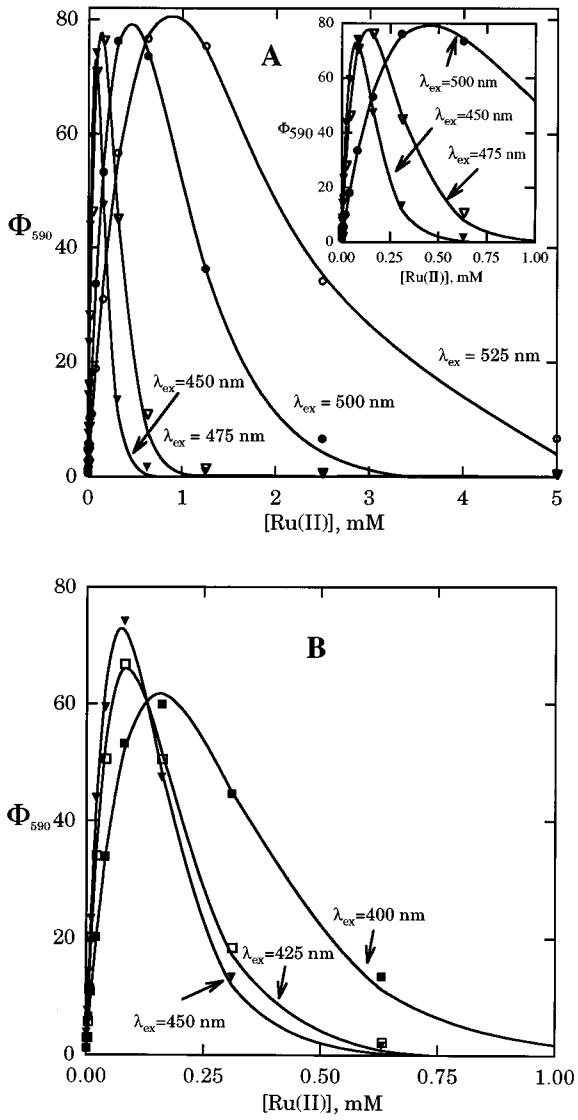

FIG. 3. Inner filter effect as a function of the wavelength of the excitation radiation. Φ_{590} is the intensity of the emitted fluorescence measured at 590 nm. (a) shows Φ_{590} for excitation wavelengths λ_{ex} at 525 nm, 500 nm, 475 nm, and 450 nm. The inset shows the details when λ_{ex} is 450 nm, 475 nm, and 500 nm at low $Ru(bpy)_3^{2+}$ concentrations. (b) shows Φ_{590} for λ_{ex} at 450 nm, 425 nm, and 400 nm. Note that in (a) the inner filter effect curves are getting more narrow as λ_{ex} goes from 525 nm to 450 nm. In (b) however, the inner filter effect curves get broader again as λ_{ex} decreases further from 450 nm to 400 nm. Open and solid symbols represent experimental data. Solid lines show the fit of experimental points to the trial function $\Phi_{590} = A_{ex}[\mathrm{Ru(II)}]e^{-B_{ex}[\mathrm{Ru(II)}]}$. For the trial function, the following (A_{ex}, B_{ex}) values were obtained for the following excitation wavelengths: 525 nm, $(2.53\times10^5\ M^{-1}, 1.16\times10^3\ M^{-1})$; 500 nm, $(4.9\times10^5\ M^{-1}, 2.26\times10^3\ M^{-1})$; 475 nm, $(1.63\times10^6\ M^{-1}, 7.68\times10^3\ M^{-1})$; 450 nm, $(2.72\times10^6\ M^{-1}, 1.37\times10^4\ M^{-1})$; 425 nm, $(2.11\times10^6\ M^{-1}, 1.17\times10^4\ M^{-1})$; 400 nm, $(1.10\times10^6\ M^{-1}, 6.53\times10^3\ M^{-1})$.

filter effect is observed. This means that Φ decreases with increasing concentration after a certain concentration in the fluorescent species has been reached.[18,19]

If we assume that *all* absorbed excitation radiation within the fluorimetric cell is converted (to a certain extent) to fluorescent radiation and measured by the instrument, the fluorescence intensity Φ should show saturating behavior

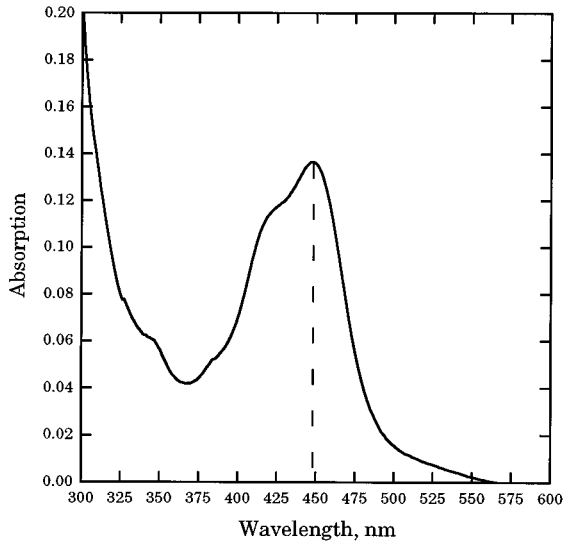

FIG. 4. Absorption spectrum of a 2×10^{-5} M $Ru(bpy)_3^{2+}$ solution in 1 M sulfuric acid.

with increasing concentration of the fluorescent compound, i.e.,[18,19]

$$\Phi = I_0 \cdot Q_f(1-10^{-\epsilon cl}), \tag{1}$$

where I_0 is the intensity of the incoming excitation beam, Q_f is the quantum yield, while ϵ is the molar absorptivity of the fluorescent compound, c is its concentration, and l is the length the beam has to travel through the absorbing (and fluorescent) medium.

However, in case of a standard orthogonal and rectangular beam/cell arrangement, the photomultiplier tube senses only *part* of the emitted fluorescence radiation. For high concentrations of the fluorescent compound, strong absorption (and fluorescence) may occur even before the excitation beam enters the measuring area of the photomultiplier. Thus, as the concentration of the fluorescent compound increases an apparent decrease in fluorescence in the measuring zone may be found. Under such conditions, Φ will depend on concentration c according to the relationship (see Appendix)

$$\Phi = 2I_0 \cdot Q_f 10^{-\epsilon cl/2} \sinh(2.303\epsilon cx), \tag{2}$$

where x is the half-width of the measuring area (see Fig. 11 in the Appendix). Only at low concentrations c, a linear relationship between Φ and c may be observed.

For the $Ru(pby)_3^{2+}$ ion, the inner filter effect is dependent on the excitation wavelength (Fig. 3). At λ_{ex}=450 nm the inner filter effect is strongest {i.e., the $\Phi_{590}-[Ru(bpy)_3^{2+}]$ curve is narrowest; see Fig. 3}, which is in agreement with that at this wavelength the absorption by $Ru(bpy)_3^{2+}$ has a maximum (Fig. 4). The strong absorption at 450 nm and the corresponding inner filter effect can also be recognized in the three-dimensional spectrum (Fig. 2); at λ_{ex}=450 nm the fluorescence intensity Φ_{590} shows a minimum.

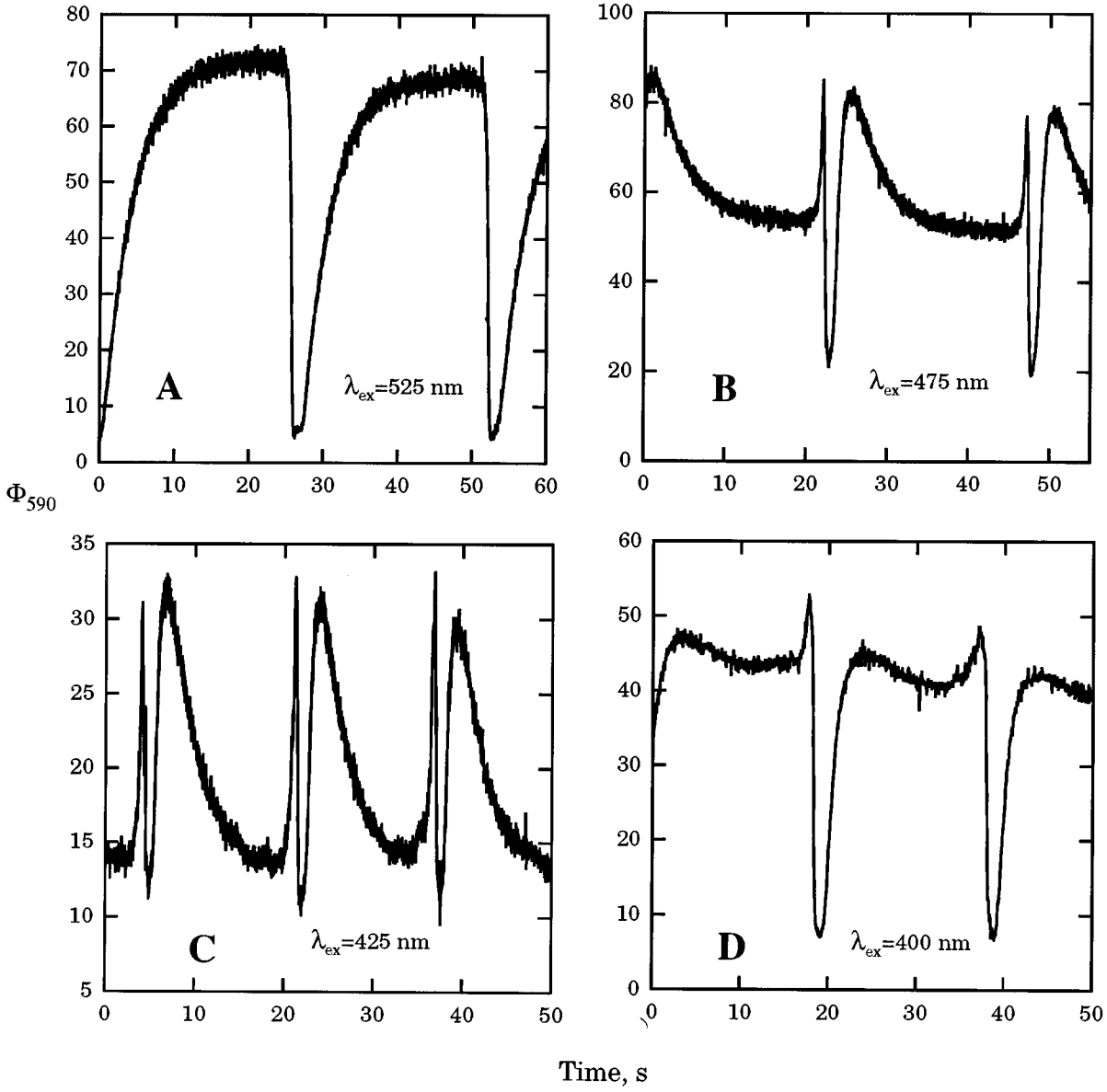

FIG. 5. (a) Different fluorescence oscillations at an emitted wavelength of 590 nm. In all cases (a)–(d) the initial Ru-ion concentration is 5×10^{-4} M. Excitation wavelengths; (a) 525 nm; (b) 475 nm; (c) 425 nm; (d) 400 nm. The oscillations were recorded approximately 5–6 min after mixing of the reagents.

B. Oscillatory behavior of fluorescence

1. Dependence of excitation wavelength

The fluorescence emission spectrum for the (oscillatory) BZ system is the same as for the isolated $Ru(bpy)_3^{2+}$ (Fig. 2) except that the fluorescence peaks are now oscillatory. A closer inspection revealed that the form of the fluorescence oscillations at 590 nm (Φ_{590}) is significantly dependent on the excitation wavelength λ_{ex}. Figure 5 shows how the form of the Φ_{590} oscillations changes as λ_{ex} is varied from 525 nm to 400 nm.

When using an initial catalyst concentration of 5×10^{-4} M, visual inspections showed that during the first 30 min of oscillation the color of the reacting solution alternated between green [oxidized form of the catalyst, i.e., $Ru(bpy)_3^{3+}$] and orange [$Ru(bpy)_3^{2+}$]. However, the green color slowly disappeared during this period and the solution remained orange, while redox oscillations' amplitude increased in the direction of a more reducing potential (i.e., towards a higher ln{[Ru(II)]/Ru(III)]} ratio). From these observations we conclude that during the oscillations the average concentration of Ru(II) increases. In fact, we will show how such an increase can explain the gradual change of the fluorescent oscillation shape at Ru-ion concentrations of 5×10^{-4} M or higher [Fig. 6(a)]. Slight differences in this behavior were found when either using the commercial $[Ru(bpy)_3]Cl_2\cdot6H_2O$ salt or when using the self-prepared sulfato salt. While in both cases the fluorescence intensity Φ_{590} is strongly damped (quenched) at higher initial Ru-ion concentrations, we found that when using $[Ru(bpy)_3]Cl_2$ the fluorescence intensity Φ_{590} became slightly more rapidly quenched in comparison with the sulfate salt.

2. Dependence of initial $Ru(bpy)_3^{2+}$ concentration

We also found that the form of the fluorescence oscillations is dependent upon the initial Ru(II) concentration. Fig-

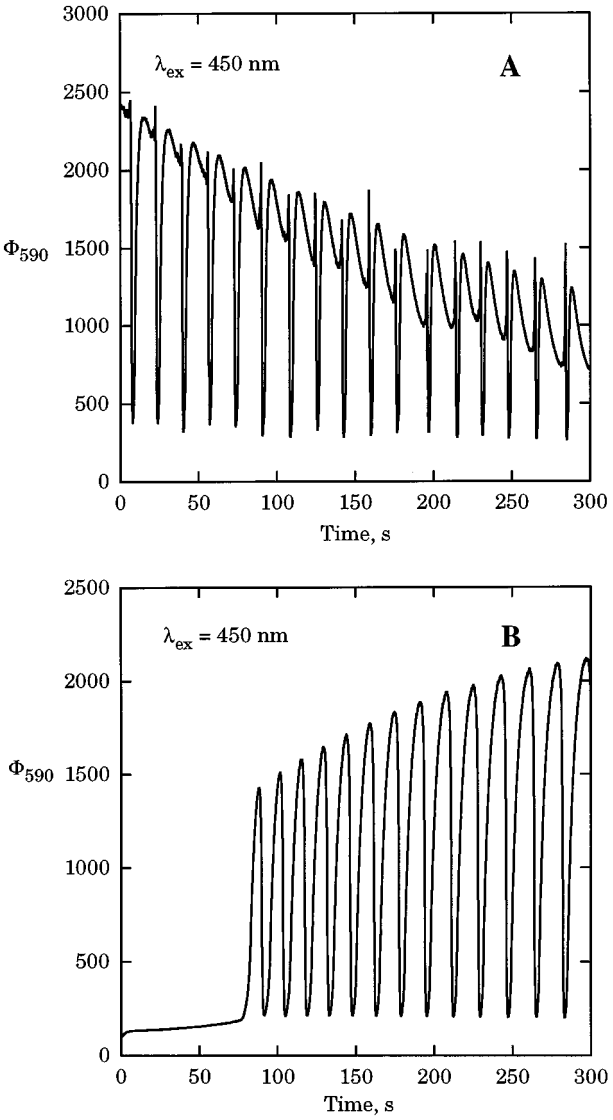

FIG. 6. (a) Damping (quenching) of fluorescence of a BZ oscillator with an initial Ru(II) concentration of 5×10^{-4} M. The excitation wavelength is 450 nm. Note the gradual change in the shape of the oscillations. (b) Same system as in (a) but with an initial Ru(II) concentration of 6×10^{-5} M. Note the appearance of an induction period.

ure 6(b) shows that when the initial Ru(II) concentration is decreased, oscillations become single-peaked. In addition, the Φ_{590} oscillations are not damped and amplitude may in fact increase with time [Fig. 6(b)]. With a decrease in the initial Ru-ion concentration, the appearance of an induction period is also observed. In accordance with other classical[21] catalyzed BZ systems,[22] the length of the induction period increases as the initial Ru-ion concentration decreases (data not shown).

C. Relationships between inner filter effect and the form of fluorescence oscillations

The reduced form of the Ru-catalyst, $Ru(bpy)_3^{2+}$, is the fluorescent species. At very low Ru(II) concentrations there is a linear relationship between fluorescence intensity Φ and [Ru(II)]. Figure 7(a) shows that under such conditions, oscillations in Ru(II) concentration will lead to corresponding

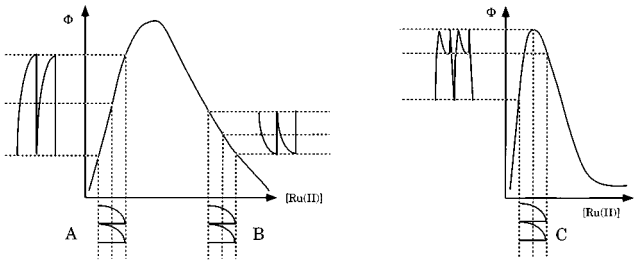

FIG. 7. Phase relationships between oscillatory Ru(II) concentration and oscillatory fluorescence intensity Φ in relation to an inner filter effect. (a) positively correlated in-phase oscillations between Φ and [Ru(II)]; (b) negatively correlated opposite-phase oscillations between Φ and [Ru(II)]; (c) complex oscillations in Φ when [Ru(II)] oscillations cover the Φ maximum of the inner filter effect curve.

in-phase oscillations in Φ, i.e., whenever [Ru(II)] in- or decreases then Φ also in- or decreases, respectively.

In the case [Ru(II)] oscillates at very high concentration values, the Φ-[Ru(II)] relationship will be on the descending branch of the inner filter effect curve [Fig. 7(b)]. In this case, an increase in the Ru(II) concentration will lead to a decrease in Φ, while a decrease in [Ru(II)] will lead to a increase in Φ. Therefore, oscillations in [Ru(II)] in such a high concentration range will lead to Φ oscillations which are in *opposite* phase to the [Ru(II)] oscillations [Fig. 7(b)].

A third alternative for the shape of Φ oscillations is possible when the range of [Ru(II)] oscillations covers the Φ-maximum in the inner filter effect curve [Fig. 7(c)]. In this case *complex* Φ oscillations are observed as the Ru(II) concentration oscillates around the Φ maximum.

D. Simulating the form of Φ_{590} oscillations as a function of excitation wavelength

A semiquantitative mathematical description of the BZ oscillations can be obtained by the Oregonator model. In its original[10] form the Oregonator consists of five pseudoelementary processes (O1)–(O5),

$$A+Y\rightarrow X+P, \tag{O1}$$

$$X+Y\rightarrow 2P, \tag{O2}$$

$$A+X\rightarrow 2X+Z, \tag{O3}$$

$$2X\rightarrow A+P, \tag{O4}$$

$$Z\rightarrow fY, \tag{O5}$$

with the rate constant values[23] $k_{O1}=1.3\ M^{-1}\,s^{-1}$, $k_{O2}=2\times10^{6}\ M^{-1}\,s^{-1}$, $k_{O3}=34\ M^{-1}\,s^{-1}$, $k_{O4}=3\times10^{3}\ M^{-1}\,s^{-1}$, $k_{O5}=0.02\ s^{-1}$. The factor f is a time constant; in the calculations here we use $f=1.0$. The concentration variable assignment is $A=BrO_3^-$, $X=HBrO_2$, $Y=Br^-$, $Z=2Ru(III)$, and $P=HOBr$. The kinetic active components are X,Y,Z with $[A]=0.1$ M.

In the Oregonator the maximum Z value is 2.65×10^{-2} M, which is much too high compared to the initial concentrations used in our experiments ($\leqslant5\times10^{-4}$ M). In order to fit the Oregonator Z-concentration values to the range used in the experiments, we consider the following scaled mass balance:

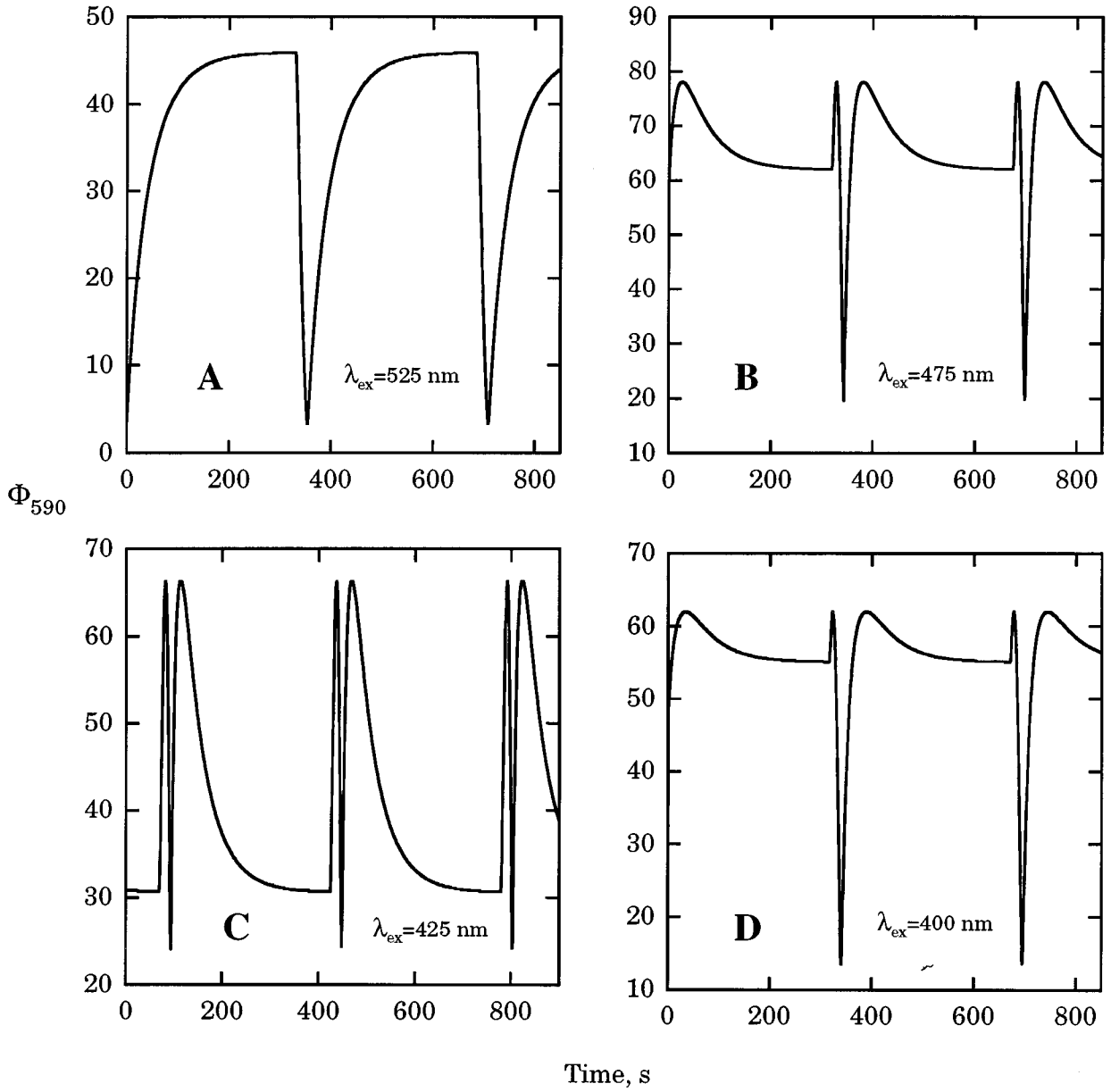

FIG. 8. Simulated Φ_{590} oscillations corresponding to the experiments of Fig. 5. The oscillations are obtained by first calculating $[C]$ from the scaled Oregonator Z values [using Eq. (3) with $\kappa=8.3\times10^{-3}$ and $[C]_0=2.4\times10^{-4}$ M]. The Φ_{590} values are obtained by inserting $[C]$ into Eq. (4). The different excitation wavelengths correspond to the following (A_{ex},B_{ex}) values: (a) $(2.53\times10^5\ M^{-1}, 1.16\times10^3\ M^{-1})$; (b) $(1.63\times10^6\ M^{-1}, 7.68\times10^3\ M^{-1})$; (c) $(2.11\times10^6\ M^{-1}, 1.17\times10^4\ M^{-1})$; (d) $(1.10\times10^6\ M^{-1}, 6.53\times10^3\ M^{-1})$.

$$[C]=[C]_0-\kappa\cdot[Z], \tag{3}$$

where $[C]_0$ corresponds to the total amount of catalyst in the system, $[C]=2[\mathrm{Ru(bpy)}_3^{2+}]$ and κ is a scaling factor. The purpose of the scaling factor is to reduce the value of $[Z]$ such that $[Z]$ lies within in the experimental range of the catalyst concentration.

C is the fluorescent species of the catalyst. The inner filter effect curves (Fig. 3) are quantitatively well described by the following simple relationship:

$$\Phi_{590}=A_{ex}[C]e^{-B_{ex}[C]}, \tag{4}$$

where A_{ex} and B_{ex} are parameters which depend on the excitation wavelength [for numerical values of (A_{ex}, B_{ex}) see legend of Fig. 3]. By inserting the numerically calculated $[C]$ values [Eq. (3)] into Eq. (4), the Oregonator is able to simulate the experimentally observed Φ_{590} oscillations.

Figure 8 shows Oregonator simulations that correspond to the experiments of Fig. 5. The agreement with experiment, although not quantitative, is quite good showing that the inner filter effect of the isolated $\mathrm{Ru(bpy)}_3^{2+}$ ion is responsible for the various Φ_{590} oscillation forms observed at different excitation wavelengths.

E. Experimental proof of in-phase and opposite-phase relationships between Φ_{590} and $[\mathrm{Ru(bpy)}_3^{2+}]$ oscillations

A direct experimental proof between in-phase and opposite-phase relationships between Φ_{590} and $[\mathrm{Ru(bpy)}_3^{2+}]$

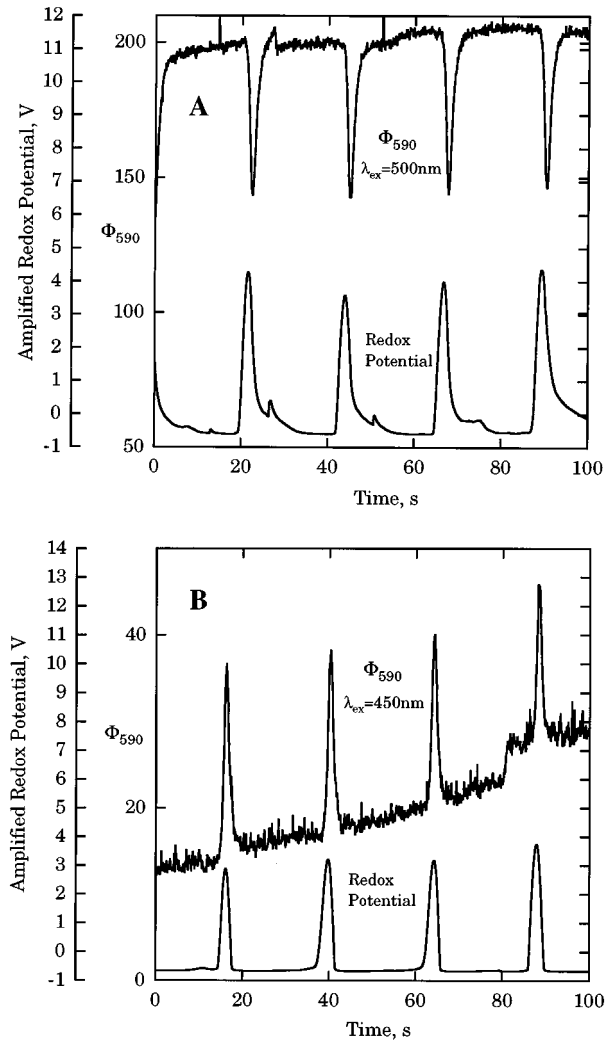

FIG. 9. (a) In-phase relationship between Φ_{590} and $[Ru(bpy)_3^{2+}]$ oscillations. λ_{ex}=500 nm and initial $[Ru(bpy)_3^{2+}]_0=5\times10^{-4}$ M. The recorded redox potential is proportional to $\ln\{[Ru(bpy)_3^{3+}]/[Ru(bpy)_3^{2+}]\}$, i.e., *oxidation spikes* (Ref. 25) are observed. A low redox potential represents high $Ru(bpy)_3^{2+}$ concentrations and high Φ_{590} values. (b) Opposite-phase relationships between oscillatory Φ_{590} and oscillatory $Ru(bpy)_3^{2+}$ concentration. λ_{ex}=450 nm and the same initial Ru(II) concentration as in (a). In this case low redox potentials represent still high $Ru(bpy)_3^{2+}$ concentrations but *low* Φ_{590} values. The oscillations were taken approximately 15 min after mixing of initial reagents. During this time the character of the oscillations changed from initially in-phase oscillations via complex oscillations [Fig. 6(a)] to the present case of opposite phase oscillations.

oscillations can be given by a simultaneous record of the redox potential oscillations and the Φ_{590} oscillations. Figure 9(a) shows positively correlated in-phase relationships between $[Ru(bpy)_3^{2+}]$ oscillations and Φ_{590} oscillations, while Fig. 9(b) shows negatively correlated opposite phase relationships between $[Ru(bpy)_3^{2+}]$ oscillations and Φ_{590} oscillations.

F. Change of Φ_{590} oscillation form with time

When using an initial $Ru(bpy)_3^{2+}$ concentration of 5×10^{-4} M (or higher) and an excitation wavelength of 450 nm (corresponding to the narrowest inner filter effect curve) a gradual change in the type of Φ_{590} oscillations can be seen. At the beginning, the Φ_{590} oscillations are in phase with the oscillations of $[Ru(bpy)_3^{2+}]$. However, at this excitation wavelength the oscillations' form change very rapidly to the complex type and finally to opposite-phase oscillations. In addition, when the initial $Ru(bpy)_3^{2+}$ concentration is 5×10^{-4} M or higher, the Φ_{590} oscillation become strongly damped [Fig. 6(a)] (which is not seen for an identical system's redox potential oscillations or absorption oscillations record at 450 nm).

We do presently not understand the mechanism that shrinks the amplitude of fluorescence oscillations and why damping of the amplitude does not take place at lower initial catalyst concentrations. While the change from in-phase to complex-phase oscillations [Fig. 6(a)] easily can be explained by a gradual increase of the Ru(II) concentration during the oscillations, the damping of the amplitude in Fig. 6(a) is not related to the inner filter effect.

In principle, oxidative, reductive, or energy transfer mechanism[24] may be responsible for the decay of the Φ_{590} amplitude. The complex chemistry of the BZ reaction offers a variety of possibilities and an El Dorado for further research.

Figure 10 is an Oregonator simulation that shows that the gradual change in phase relationships between Φ_{590} and Ru(II) oscillations is due to a gradual increase in the Ru(II) concentration. To mimick the damping of the amplitude an empirical damping factor $f_{\text{damp}} = e^{-k_{\text{damp}}t}$ was included.

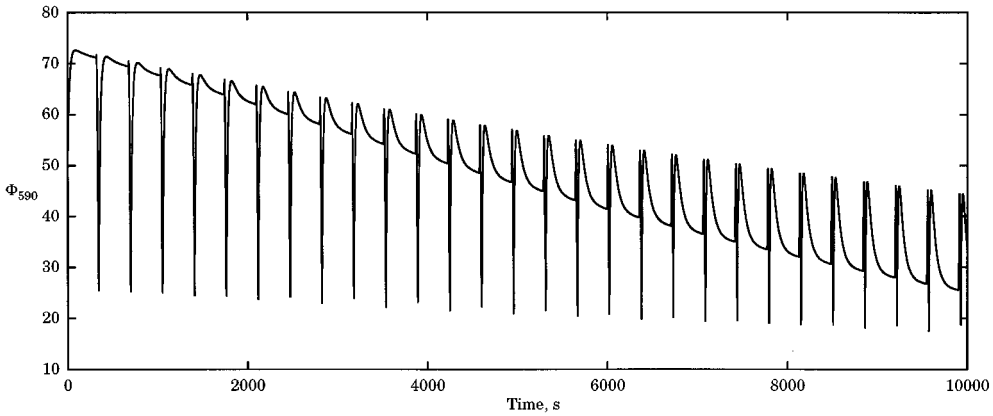

FIG. 10. Simulation of Φ_{590} oscillations for initial $Ru(bpy)_3^{2+}$ concentrations of 5×10^{-4} M or higher. The damping of the amplitude is described by a damping factor $f_{\text{damp}} = e^{-k_{\text{damp}}\cdot t}$ with $\Phi_{590} = f_{\text{damp}} \cdot A_{\text{ex}}[C]e^{-B_{\text{ex}}[C]}$. The change of the oscillatory waveform is due to an increase in $[C]$ which is described by an increase in $[C]_0(t)$ according to $[C]_0(t)=[C]_0(0)+a\cdot t$. The scaling factor κ is calculated by $\kappa=\{[C]_0(t)-[C]_{\min}/[Z]_{\max}\}$. The numerical values of the parameters are $k_{\text{damp}}=5\times10^{-5}$ s^{-1}; $A_{\text{ex}}=2.72\times10^{6}$ M^{-1}; $B_{\text{ex}}=1.37\times10^{4}$ M^{-1}; $[C]_0(0)=8\times10^{-5}$ M; $a=1\times10^{-8}$ M s^{-1}.

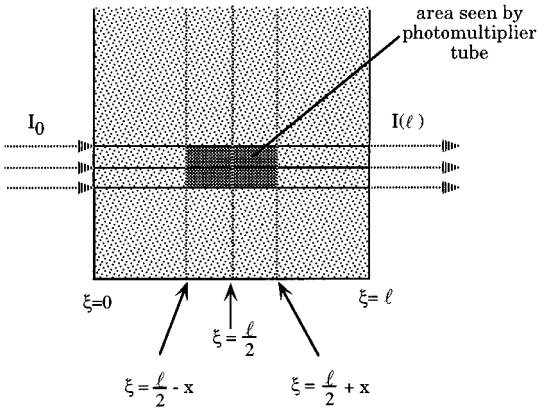

FIG. 11. Schematic drawing of fluorescent solution inside fluorimetric cell with light path length l. The inner filter effect is due to the fact that only a part of the light path [starting from $\xi=(l/2)-x$ to $\xi=(l/2)+x$] is recognized by the photomultiplier.

The increase in the Φ_{590} amplitude at lower initial Ru(II) concentrations is in agreement with corresponding increases in amplitude for identical systems which are studied by potentiometry or spectrophotometry. These increases in amplitude reflect the general concentration increase in the reduced form of the catalyst.

G. Difficulties in interpreting oscillatory fluorescence

When using standard fluorimetric equipment with rectangular cell geometries and an orthogonal beam arrangement an inner filter effect can be expected whenever the concentration of the fluorescent species exceeds a certain concentration.[18,19] As our results show, an inner filter effect will make it difficult to evaluate the phase relationship between the oscillatory species and the observed fluorescence from oscillatory Φ records only. Furthermore, correct estimates of concentration values of the fluorescent species may also be difficult to obtain, mostly due to the highly quenching environment in the BZ reaction.[15]

ACKNOWLEDGMENT

G.M.S. thanks the Department of Physical Chemistry, Norwegian Institute of Technology, for allowing us to conduct this research at Stavanger College.

APPENDIX

We derive here Eq. 2. $I(\xi)$ denotes the intensity of the excitation beam at location ξ in the cell (Fig. 11). According to Lambert–Beers law, we can write $I(\xi)=I_0 10^{-\epsilon c \xi}$ with $I_0=I(0)$.

Let us assume that the area covered by the photomultiplier tube starts at $\xi=(l/2)-x$ and ends at $\xi=(l/2)+x$, where l is the length of the light path in the cell (Fig. 11). The amount of absorbed radiation within the sensing area is

$$
\begin{aligned}
I_a^{\text{meas}} &= I\left(\frac{l}{2}-x\right)-I\left(\frac{l}{2}+x\right) \\
&= I_0[10^{-\epsilon c(l/2-x)}-10^{-\epsilon c(l/2+x)}] \\
&= 2I_0 10^{-\epsilon c l/2}\left(\frac{e^{-\epsilon c x \ln 10}-e^{-\epsilon c x \ln 10}}{2}\right) \\
&= 2I_0 10^{-\epsilon c l/2} \sinh(\epsilon c x \ln 10).
\end{aligned}
$$

Since $\Phi = Q_f I_a^{\text{meas}}$, we get Eq. (2),

$$\Phi = 2I_0 Q_f 10^{-\epsilon c l/2} \sinh(\epsilon c x \ln 10).$$

[1] B. P. Belousov, in *Oscillations and Traveling Waves in Chemical Systems*, edited by R. J. Field and M. Burger (Wiley, New York, 1985).
[2] A. M. Zhabotinsky, in *Oscillations and Traveling Waves in Chemical Systems*, edited by R. J. Field and M. Burger (Wiley, New York, 1985).
[3] (a) R. J. Field, in *Oscillations and Traveling Waves in Chemical Systems*, edited by R. J. Field and M. Burger (Wiley, New York, 1985); (b) R. M. Noyes and R. J. Field, Annu. Rev. Phys. Chem. **25**, 95 (1974); (c) R. J. Field, in *Theoretical Chemistry*, edited by H. Eyring and D. Henderson (Academic, New York, 1978), Vol. 4; (d) P. Gray and S. K. Scott, *Chemical Oscillations and Instabilities* (Clarendon, Oxford, 1990), Chap. 14.
[4] (a) P. Ruoff, Chem. Phys. Lett. **90**, 76 (1982); (b) **92**, 239 (1982); (c) **96**, 374 (1983).
[5] (a) A. N. Zaikin and A. M. Zhabotinsky, Nature **225**, 535 (1970); (b) A. T. Winfree, Science **175**, 634 (1972); (c) P. Ruoff, Naturwissenschaften **70**, 306 (1983); (d) in *Spatial Inhomogeneities and Transient Behaviour in Chemical Kinetics*, edited by P. Gray, G. Nicolis, F. Baras, P. Borckmans, and S. K. Scott (Manchester University, Manchester, 1990); (e) in *Waves and Patterns in Chemical and Biological Media*, edited by H. L. Swinney and V. I. Krinsky (North-Holland, Amsterdam, 1991).
[6] (a) W. Geiseler and H. H. Föllner, *Biophys. Chem.* **6**, 107 (1977); (b) W. Geiseler and K. Bar-Eli, J. Phys. Chem. **85**, 908 (1981); (c) P. Ruoff and R. M. Noyes, *ibid*. **89**, 1339 (1985).
[7] *Nonlinear Phenomena in Chemical Dynamics*, edited by C. Vidal and A. Pacault (Springer, Berlin, 1981).
[8] S. K. Scott, *Chemical Chaos* (Clarendon, Oxford, 1991).
[9] (a) R. M. Noyes, R. J. Field, and E. Körös, J. Am. Chem. Soc. **94**, 1394 (1972); (b) R. J. Field, E. Körös, and R. M. Noyes, *ibid*. **94**, 8649 (1972).
[10] R. J. Field, and R. M. Noyes, J. Chem. Phys. **60**, 1877 (1974).
[11] (a) R. M. Noyes, in *Synergetics. Far from Equilibrium*, edited by A. Pacault and C. Vidal (Springer, Berlin, 1979); (b) K. Showalter, R. M. Noyes, and K. Bar-Eli, J. Chem. Phys. **69**, 2514 (1978); (c) R. J. Field, *ibid*. **63**, 2289 (1975); **65**, 1603 (1976); (d) P. Ruoff and R. M. Noyes, *ibid*. **84**, 1413 (1986).
[12] J. N. Demas and D. Diemente, J. Chem. Educ. **50**, 357 (1973).
[13] (a) L. Kuhnert, Nature **319**, 393 (1986); (b) M. Jinguij, M. Ishihara, and T. Nakazawa, J. Phys. Chem. **94**, 1226 (1990); **96**, 4279 (1992); (c) M. K. Ram Reddy, Zs. Nagy-Ungvarai, and S. C. Müller, *ibid*. **98**, 12 255 (1994).
[14] F. Bolletta and V. Balzani, J. Am. Chem. Soc. **104**, 4250 (1982).
[15] P. Ruoff, Chem. Phys. Lett. **226**, 295 (1994).
[16] (a) Z. Varadi and M. T. Beck, J. Chem. Soc. Chem. Commun. **1973** 30; (b) S. Jacobs and I. R. Epstein, J. Am. Chem. Soc. **98**, 1721 (1976); (c) M. Mrakavova and L. Treindl, Coll. Czech. Chem. Commun. **51**, 2693 (1986); (d) S. Murányi and H.-D. Försterling, Z. Naturforsch. **45a**, 135 (1990).
[17] Y. Gao and H.-D. Försterling (preprint).
[18] *Spectrophotometry & Spectrofluorimetry*, edited by D. A. Harris and C. L. Bashford (IRL, Oxford, 1987).
[19] D. Rendell, *Fluorescence and Phosphorescence* (Wiley, Chicester, 1987).
[20] A. C. Hindmarsh, ACM-SIGNUM Newsletter **15**, 10 (1980).
[21] R. M. Noyes, J. Am. Chem. Soc. **102**, 4644 (1980).
[22] P. Ruoff and B. Z. Schwitters, Phys. Chem. (Wiesbaden) **135**, 171 (1983).
[23] R. J. Field and H.-D. Försterling, J. Phys. Chem. **90**, 5400 (1986).
[24] R. J. Watts, J. Chem. Educ. **60**, 834 (1983).
[25] P. Ruoff and R. M. Noyes, J. Chem. Phys. **89**, 2696 (1988).